Available online at www.sciencedirect.com
ScienceDirect
Ceramics International 36 (2010) 923–927
CERAMICS INTERNATIONAL
www.elsevier.com/locate/ceramint

Cellular silica-based ceramics prepared by direct foaming at high temperature

Changming Xu [a,b,*], Shiwei Wang [a], Katarina Flodström [b], Xiaojian Mao [a], Jingkun Guo [a]

[a] Shanghai Institute of Ceramics, Chinese Academy of Sciences, 1295 Dingxi Road, Shanghai 200050, People's Republic of China
[b] Department of Inorganic Chemistry, Arrhenius Laboratory, Stockholm University, S-106 91 Stockholm, Sweden

Received 1 September 2009; received in revised form 16 September 2009; accepted 20 October 2009
Available online 20 November 2009

Abstract

Cellular silica-based ceramics, including Si_3N_4/SiO_2 composite ceramics and monolithic silica ceramics, with dense shell and closed cells with dense and crack-free cell wall inside was prepared by the direct foaming of the green-compacts at 1310–1370 °C. The influences of the heat-treatment temperature on the relative density as well as the mechanism of the cell formation were investigated. The porosity of the obtained cellular silica and Si_3N_4/SiO_2 ceramics was within 60.0–84.0%, the cell size distribution was in the range of 10–120 μm, and the flexural strength was 9.7–16.3 MPa.

Keywords: Cellular; Silica-based ceramics; Direct foaming

1. Introduction

Silica ceramics as well as its composite ceramics reinforced with Si_3N_4 [1–3], AlN [4], BN [5] particle and silica fiber [6,7] have excellent dielectric properties and thermal-shock resistance, low thermal conductivity and thermal expansion coefficient, making them promising candidates for high-temperature dielectric and thermal-shielding application in aero craft in the recent decades. In order to expand their application under more rigorous conditions, the introduction of cells into the silica-based ceramics is desirable, owing to the fact that the existence of cells in ceramics can effectively decrease the dielectric constant, thermal conductivity, and specific weight [8–11].

By far, cellular ceramics with adjustable cell size, shape, and porosity can be prepared by the processing techniques of replica, sacrificial template, and direct foaming techniques [9]. However, organic templates for the cellular structure formation or agents for the generation of gas and/or liquid are usually required for the fabrication of cellular ceramics, which brings impurities into the products or does harm to the mechanical properties. In addition, open cell silica-based structure can absorb moisture, which is detrimental for the dielectric constant [12,13].

To the best of our knowledge, studies on the preparation of cellular ceramics with high porosity and closed cell have been reported only very recently [14,15]. In this study, we report the preparation of cellular silica-based ceramics, including Si_3N_4/SiO_2 composite ceramics and monolithic silica ceramics with high porosity and high mechanical properties such as flexural strength by the direct foaming of green-compact at high temperature. The influence of the heat-treatment temperature on the porosity of the resultant sintered-body was studied and the cell formation mechanism was investigated.

2. Experimental procedure

Silica powders and Si_3N_4/SiO_2 composite powders were prepared with sol–gel method. All of the chemicals used in present study were in chemical purity. α-Si_3N_4 powders (UBE-10, UBE Industry Co., Ltd., Japan), with an average diameter of 0.5 μm were also used to prepare Si_3N_4/SiO_2 composite powders. The processing route for Si_3N_4/SiO_2 composite powders as well as monolithic silica gel powders was illustrated in Fig. 1. Firstly, silica sol was prepared by mixing

* Corresponding author at: Shanghai Institute of Ceramics, Chinese Academy of Sciences, 1295 Dingxi Road, Shanghai 200050, People's Republic of China.
E-mail address: charmingxu@hotmail.com (C. Xu).

0272-8842/$36.00
doi:10.1016/j.ceramint.2009.10.023

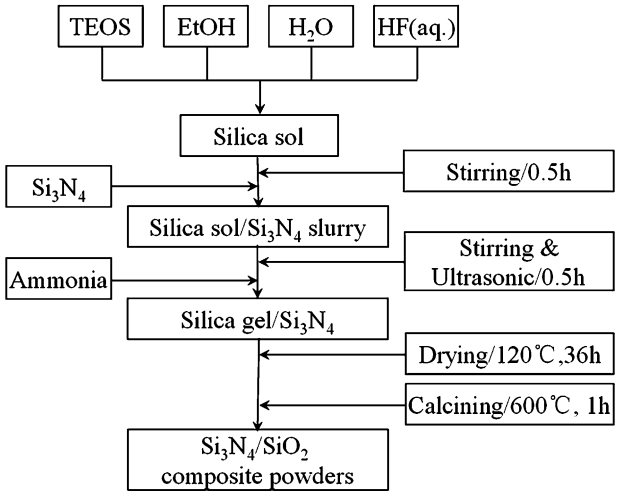

Fig. 1. Sol–gel processing route for the Si_3N_4/SiO_2 composite powder. Silica monolithic gel powders can also be prepared with this method without adding Si_3N_4 powders.

tetraethoxysilane (TEOS), ethanol (EtOH), deioned-water, and HF aqueous solution with the molar ratio of TEOS:EtOH:-H_2O:HF = 1:5:3:0.03 together. After stirred at room temperature for 0.5 h, the Si_3N_4 powders with 10 wt.% based on solids, was added into the mixture solutions. After ultrasonic treatment with simultaneously and vigorously stirring for another 0.5 h, the mixture was then added rapidly with sufficient ammonia till the complete accomplishment of the gellization. Silica gel with Si_3N_4 powder uniformly dispersed inside was therefore quickly formed. The composite gel was dried at 120 °C for 36 h and then calcined at 600 °C for 1 h. Silica gel without adding Si_3N_4 powder was also prepared by this method at the same time.

The obtained silica-based powders were dry-pressed into 40 mm × 60 mm green-compacts with ∼60 MPa pressure without any binder added, and followed by cold isostatic pressing with ∼200 MPa pressure, respectively. The green-compacts were then heat-treated at 1100–1370 °C for 2 h in an air atmosphere at a rate of 10 °C min^{-1}.

The morphology of the Si_3N_4/SiO_2 composite powders was observed by transmission electron microscopy (TEM, JEM2100F, JEOL, Tokyo, Japan). The phase composition of the sintered compacts was identified by X-ray diffraction (XRD, D/max 2550 V, Rigaku Co., Tokyo, Japan). The microstructure of the resultant ceramics was observed by scanning electron microscopy (SEM, JSM6700F, JEOL, Tokyo, Japan). Flexural strength was measured using an Instron-1195 universal testing machine (Satec Co., Port Monmouth, USA) with a cross head speed of 1 mm s^{-1}. The inner fraction of the samples was cut into test pieces with a dimension of 5 mm × 5 mm × 40 mm. The cross-sectional area of the samples and the maximum failure load were used to calculate the fracture stress. The density of the whole sintered-body was measured by the Archimedes' method. After the measurement, the outer part of the samples was cut-off so that the density of the inner part of the sample can be measured by the same method. The Fourier transform infrared (FTIR) spectra were obtained using a Nicolet NEXUS 7000-C spectrometer with a 4 cm^{-1} resolution.

3. Results and discussion

3.1. Composite powders characterization

The morphology of the Si_3N_4/SiO_2 composite powders was shown in Fig. 2. Without serious hard agglomeration, the Si_3N_4 particles generally disperse well in the silica gel and most of the Si_3N_4 particles were surrounded by silica gel particles with a much less average particle diameter.

3.2. Sintering behavior, phase composition, and microstructure observation

Fig. 3 shows the relationships between the shrinkage of the relative density and XRD pattern (lower-left inset) of the Si_3N_4/SiO_2 ceramics and sintering temperature. The relative density of the samples was about 96.0% when heat-treated below 1200 °C for 2 h, however, decreased considerably to 33.0–40.0% and then kept stable when the temperature was increased above 1200 °C, which indicates a cell formation in the Si_3N_4/SiO_2 ceramics when heat-treated at increasing temperature.

From the XRD pattern, it can be observed that, although the Si_3N_4/SiO_2 green-compacts were subjected to an oxidative atmosphere at high temperature, α-Si_3N_4 diffraction peaks were found from the XRD patterns, which demonstrated the existence of α-Si_3N_4 phase in the resultant ceramics. Besides, trace cristobalite was detected as well in the ceramics when the heat-treatment temperature reached up to 1370 °C, which can be ascribed to the crystallization of the silica matrix at the temperature usually higher than 1350 °C [16] or partially from the oxidation of the α-Si_3N_4 particles [2].

The fact that the Si_3N_4/SiO_2 sample heat-treated at 1340 °C can float on water (see upper-right inset of Fig. 3) demonstrates the microstructure of the Si_3N_4/SiO_2 ceramics with a cellular inner fraction and dense outer shell. The apparent porosity of this sample was calculated to be 60.0% and the porosity of the

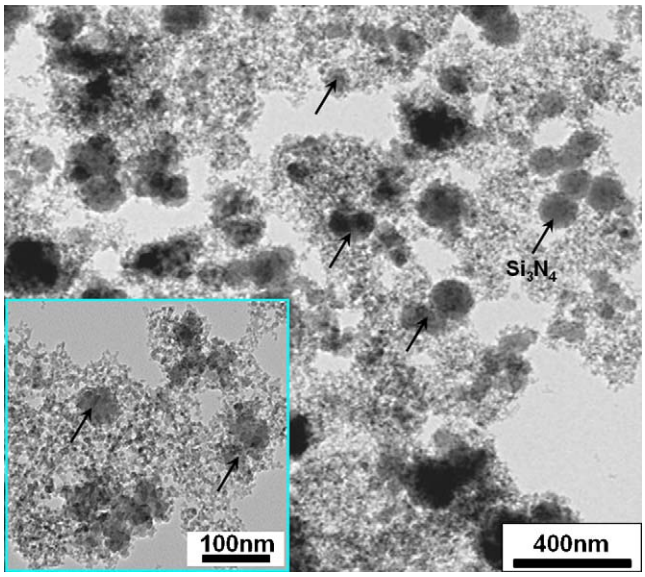

Fig. 2. TEM image of the Si_3N_4/SiO_2 composite powder.

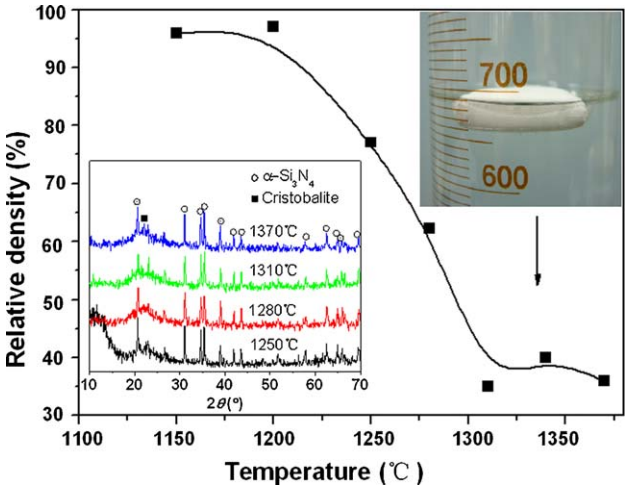

Fig. 3. Relative density and XRD pattern (lower-left inset) as a function of heat-treatment temperature. The upper-right inset shows the cellular Si_3N_4/SiO_2 ceramics heat-treated at 1340 °C floating in the water in a measuring cylinder. The porosity of the sample was 60.0% and the flexural strength was about 15.2 MPa.

inner part was 84.0% based on the relative density value. The flexural strength was about 15.2 MPa, which is remarkably higher than a previously reported strength of 2.4 MPa, in the report of which, the porosity and average pore size of the silica foam was 84% and 140 μm, respectively [17]. The flexural strength of the cellular Si_3N_4/SiO_2 ceramics heat-treated at 1300–1370 °C was in the range of 9.7–16.3 MPa. The high flexural strength could possibly be ascribed to the enhancement effect of Si_3N_4 particles in the ceramics. The dispersion of Si_3N_4 particles in the silica matrix can somewhat prevent the propagation of cracks induced by the high external load, making the cracks deflected from the initial direction, by means of which, the flexural strength of the silica can be retained by the introduction of Si_3N_4 particles.

Fig. 4 shows the microstructure of the cellular Si_3N_4/SiO_2 ceramics (Fig. 4(a–c)) and the cellular silica ceramics (Fig. 4(d)) heat-treated at 1340 °C for 2 h, respectively. There are numerous closed cells (we call it *first-ordered* cells) with a size ranging from about 10 μm to 70 μm in the inner part of the cellular Si_3N_4/SiO_2 ceramics, as shown in Fig. 4(a). The cell wall was fully dense and no cracks can be observed (Fig. 4(b)),

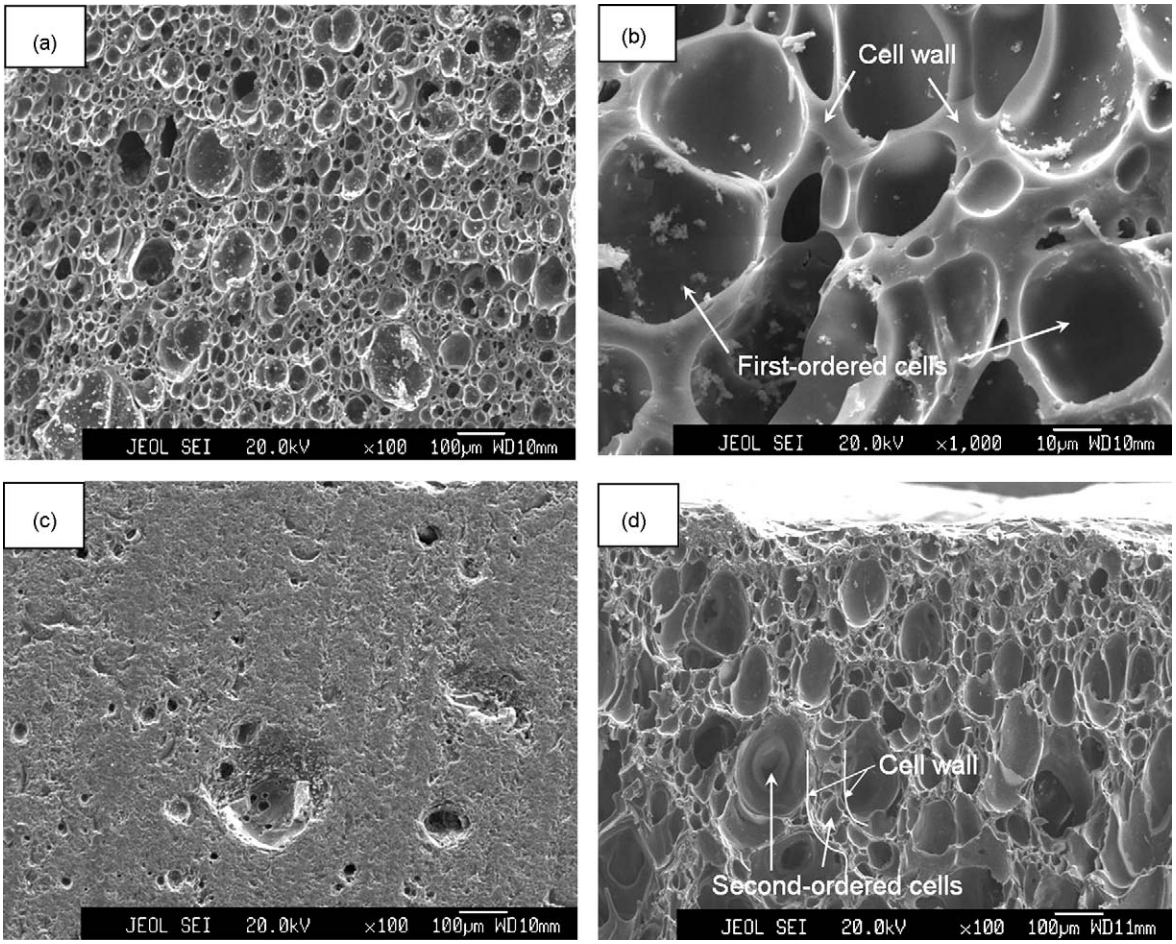

Fig. 4. Microstructure observation on different part of the cellular Si_3N_4/SiO_2 ceramics and cellular silica ceramics heat-treated at 1340 °C for 2 h under different resolutions: (a) inner fraction, lower resolution, (b) inner fraction, higher resolution, (c) outer fraction, and (d) cellular silica ceramics, the porosity is 83.0%, the flexural strength is about 9.7 MPa.

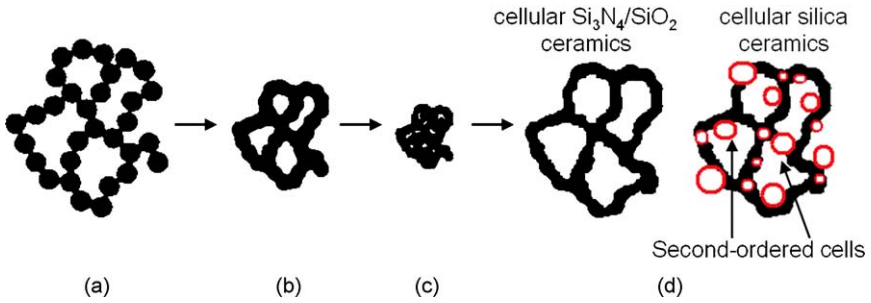

Fig. 5. Structure evaluation of the silica gel and its green-compact vs. the increasing heat-treatment temperature.

which could be another important factor that contributes, to the high flexural strength. Although some closed cells can be found (Fig. 4(c)), the outer shell of the samples were almost fully densified, which can possibly prevent the permeation of ambient moisture and/or water from outside (see upper-right inset of Fig. 3) and therefore avoiding the decline of the dielectric properties. Fig. 4(d) shows a similar cellular structure of the silica cellular ceramics except that many smaller broken cells (we call it *second-ordered* cells) appeared in the cross-section of the cell wall. The cell size distribution of the cellular silica ceramics was in the range of 20–120 μm, the porosity was about 83.0%, and the flexural strength was 9.7 MPa, which is much lower than that of the cellular Si_3N_4/SiO_2 ceramics obtained under the same conditions.

3.3. Investigation for the mechanism of the cell formation

According to the above results, the formation of the cellular ceramics can obviously be considered including three stages during the heat treatment: firstly, the silica-based green-compacts became nearly fully densified in a lower temperature range; secondly, bubbles generated in the fully densified sintered-body in a higher temperature range and the bubbles were then trapped in the inner fraction of the sintered-body after being cooled down.

Fig. 5 illustrates the structure change of the silica gel corresponding to the different heat-treatment stage. During the heat treatment of silica gel in a relatively low temperature range, most of the hydroxyl group debonded from the loose silica network as water, which can be described by the following reaction:

$$\equiv Si-OH + \equiv Si-OH \rightarrow \equiv Si-O-Si\equiv + H_2O \quad (1)$$

Therefore, the network of silica gel became denser (schemed as inset (a) to inset (b) of Fig. 5). The water released out through the interspaces of the green-compact before fully densified. Although most of the surface hydroxyl groups debonded from the silica network at low temperature, it still happens up to high temperature. This has been partially confirmed by the FTIR characterization of the Si_3N_4/SiO_2 sample heat-treated at 1200 °C, as shown in Fig. 6.

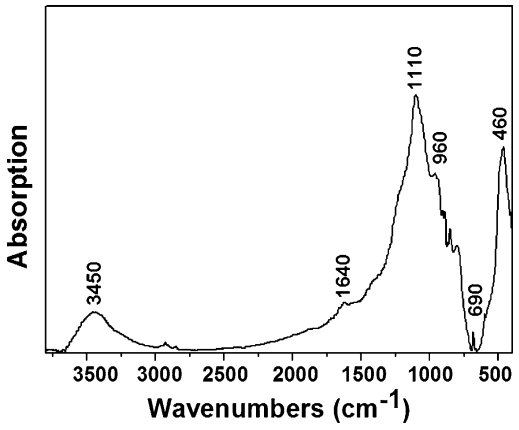

Fig. 6. FTIR spectrum of the Si_3N_4/SiO_2 sample heat-treated at 1200 °C for 2 h.

As is known, the 3440 cm^{-1} peak can be ascribed to the hydrogen-bonded water and OH stretching vibration and the 1640 cm^{-1} peak is usually attributed to the H–O–H bending vibrations. The 960 cm^{-1} shoulder peak can be assigned to the symmetric stretching vibration of the Si–OH groups [18]. The absorption peak at 480 cm^{-1} can be attributed to the lattice and O–Si–O bending vibration, the 790 cm^{-1} peak can be attributed to symmetric Si–O–Si stretching vibration, and 1100 cm^{-1} are assigned to the antisymmetric Si–O–Si stretching vibration of silica. The 620 cm^{-1} absorption peak can be assigned to E IR-active mode in the crystalline phase of cristobalite, which originates from the oxidized Si_3N_4 particle [19].

With the temperature increasing up to about 1200 °C (see Fig. 3), the shrinkage of the sintered-body was increased dramatically and then became nearly fully densified (see inset (c) of Fig. 5). It is considered that three factors were responsible for the densification of the silica-based green-compact: firstly, the existence of surface hydroxyl groups of silica gel can lead to the reduction of the viscosity at high temperature [20,21] and therefore promotes the plastic flow of the silica green-compact; secondly, the high sintering-activity of the nano-sized silica gel powders also contributed to the fast densification of silica gel green-compact. Besides, regarding the Si_3N_4/SiO_2 green-compact, the silica gel surrounding around the Si_3N_4 particles also contributed to the densification of the Si_3N_4/SiO_2 green-compact owing to the mechanism of transient viscous sintering [22]. Thus, the shrinkage can be greatly increased and the silica gel compact became nearly fully densified. This is in accordance with the experimental facts that the relative density of the Si_3N_4/SiO_2 sintered-body reached maximum value (~97.1%) at 1200 °C, as shown in Fig. 3.

Mentioned above, although heat-treated at the temperature above 1200 °C, the water stream keeps releasing in the nearly densified sintered-body and the bubbles were therefore in situ formed inside the green-body and grew up with a suppression of the surface tension of the green-compact. In case of the bubbles in the outer fraction of the sintered-body, it was much easier than that of the inner one to get broken and then released out because of the temperature gradient in the sintered-body. The bubbles can be stabilized in the sintered-body when it was cooled down to the room temperature. Cellular Si_3N_4/SiO_2 ceramics were therefore obtained. This can be confirmed by the microstructure observation of the silica cellular ceramics. From Fig. 4(d) it can be found that, the cells structure in the silica cellular ceramics was more complex than that in the Si_3N_4/SiO_2 cellular ceramics and many *second-ordered* cells can be observed not only in the cross-section of the cell wall but also on the cell surface in the silica cellular ceramics. The lower viscosity of the silica gel than that of Si_3N_4/SiO_2 green-compact made it easier for bubbles to generate and grow up in the cell wall and break up (see inset of Fig. 5(d)).

4. Conclusions

Cellular Si_3N_4/SiO_2 and monolithic silica ceramics were prepared by direct foaming the green-compacts at the temperature higher than 1300 °C. The resultant ceramics showed dense shell outside and uniformly and closed cell with crack-free cell wall inside. The porosity of the resultant cellular Si_3N_4/SiO_2 ceramics heat-treated at 1340 °C for 2 h in air was 60.0–84.0%; the cell size was in the range of 20–120 μm, the flexural strength was 9.7–16.3 MPa.

References

[1] J.J. Yao, B.S. Li, J. Inorg. Mater. 12 (1997) 47.
[2] C. Xu, S. Wang, X. Huang, J. Guo, J. Inorg. Mater. 21 (2006) 935.
[3] M. Yoshimura, T. Noma, H. Ogasawara, S. Somiya, J. Mater. Sci. Lett. 9 (1990) 53.
[4] J.-H. Wu, J.-K. Guo, B.-S. Li, J. Mater. Sci. 35 (2000) 4895.
[5] G. Wen, G.L. Wu, T.Q. Lei, Y. Zhou, Z.X. Guo, J. Eur. Ceram. Soc. 20 (2000) 1923.
[6] J. Lyons, T.L. Starr, J. Am. Ceram. Soc. 77 (1994) 1673.
[7] F.P. Meyer, G.D. Quinn, J.C. Walck, Ceram. Eng. Sci. Proc. 6 (1986) 646.
[8] C.W. Newquist, A.M. Pfister, A.D. Miller, W.D. Scott, Ceram. Bull. 60 (1981) 1205–1209.
[9] A.R. Studart, U.T. Gonzenbach, E. Tervoot, L.J. Gaucker, J. Am. Ceram. Soc. 89 (2006) 1771.
[10] S. Yu, T.K.S. Wong, X. Hu, T.K. Goh, Thin Solid Films 462–463 (2006) 311.
[11] W. Cho, R. Saxena, O. Rodriguez, R. Achanta, J.L. Plawsky, W.N. Gill, J. Non-Cryst. Solids 350 (2004) 336.
[12] Y. Uchida, S. Hishiya, N. Fujii, K. Kohmura, T. Nakayama, H. Tanaka, T. Kikkawa, Microelectron. Eng. 83 (2006) 2126.
[13] C.-T. Wang, C.-L. Wu, Thin Solid Films 496 (2006) 658.
[14] P. Colombo, E. Bernardo, Compos. Sci. Technol. 63 (2003) 2353.
[15] E. Bernardo, F. Albertini, Ceram. Int. 32 (2006) 603.
[16] C.-M. Xu, S.W. Wang, X.X. Huang, J.K. Guo, Ceram. Int. 33 (2007) 669.
[17] T. Tomita, S. Kawasaki, K. Okada, J. Porous Mater. 11 (2004) 107.
[18] C.M. Xu, S.W. Wang, M. Nogami, G.H. Zhou, H.P. Zhu, J. Am. Ceram. Soc. 10 (2007) 3268.
[19] C.M. Xu, S.W. Wang, X.X. Huang, J.K. Guo, J. Mater. Res. 20 (2005) 1943.
[20] K. Yamahara, K. Shima, A. Utsunomiya, Y. Tsurita, J. Non-Cryst. Solids 349 (2004) 341.
[21] V.K. Leko, E.V. Meshcheryakova, H.K. Gusakova, P.B. Lebedeva, Stekloi Keramika 8 (1973) 16.
[22] M.D. Sacks, Y.J. Lin, G.W. Scheiffele, K. Wang, N. Bozkurt, J. Am. Ceram. Soc. 78 (1995) 2897.